Cancer Management and Research

Dovepress

open access to scientific and medical research

Open Access Full Text Article

ORIGINAL RESEARCH

Circ_LDLR Knockdown Suppresses Progression of Hepatocellular Carcinoma via Modulating miR-7/RNF38 Axis

This article was published in the following Dove Press journal:
Cancer Management and Research

Yuming Jia
Shengchao Li
Meng Zhang
Zhilei Zhang
Chao Wang
Chong Zhang
Wuhan Yang
Li Peng
Zhuo Xu

Department of Hepatobiliary Surgery, Fourth Hospital of Hebei Medical University, Shijiazhuang 050035, Hebei, People's Republic of China

Background: Hepatocellular carcinoma (HCC) is a horrible malignancy derived from liver. Circular RNAs (circRNAs) act important roles in the pathogenesis and progression of human diseases, including HCC. The current assay intended to investigate the function of circRNA low-density lipoprotein receptor (circ_LDLR) in HCC and clarify the underlying mechanism.

Materials and Methods: Expression of circ_LDLR, microRNA (miR)-7 and ring finger protein 38 (RNF38) was determined by quantitative real-time PCR (qRT-PCR) or Western blot analysis. Flow cytometry was used to detect cell cycle distribution and apoptosis. Cell colony formation ability and viability were examined by colony formation and methyl thiazolyl tetrazolium (MTT) assays, respectively. Levels of cell proliferation and epithelia-mesenchymal transition (EMT) biomarker proteins were analyzed via Western blot assay. Cell migration and invasion were monitored by Transwell assay, and target relationship between miR-7 and circ_LDLR or RNF38 was validated by dual-luciferase reporter assay. Xenograft model was established to explore the role of circ_LDLR in vivo.

Results: Expression of circ_LDLR and RNF38 was upregulated, but miR-7 expression was downregulated in HCC tissues and cells. Circ_LDLR knockdown significantly inhibited cell proliferation, migration, invasion and EMT in HCC cells. Circ_LDLR acted as a sponge of miR-7, and interference of miR-7 could attenuate circ_LDLR knockdown-induced inhibitory effects on malignant behaviors of HCC cells. Besides, miR-7 also repressed cell proliferation and metastasis of HCC cells, by targeting RNF38. Depletion of circ_LDLR could suppress tumor growth in vivo.

Conclusion: Depletion of circ_LDLR restrained HCC cell proliferation, metastasis and tumorigenesis through the regulation on miR-7/RNF38 axis, affording a promising therapeutic target for HCC.

Keywords: HCC, circ_LDLR, miR-7, RNF38, progression

Introduction

Hepatocellular carcinoma (HCC) is the most common form among cancers derived from liver, and ranks as the third most lethiferous cancer in the world.[1] HCC is mainly resulted from infection by hepatitis B virus or chronic hepatitis C virus, or alcoholic cirrhosis.[2] Usual treatment approaches for HCC including surgical resection liver transplantation, chemotherapy and radiotherapy make a difference, while metastasis and recurrence still block the treatment of HCC.[3,4] Therefore, identifying novel biomarkers for diagnosis and metastasis is of great significance.

With covalently closed structure, circular RNAs (circRNAs) are a novel category of non-coding RNAs, which were generated from splicing errors.[5] Accumulating

Correspondence: Zhuo Xu
Department of Hepatobiliary Surgery, Fourth Hospital of Hebei Medical University, No. 169 Tianshan Street, Shijiazhuang, Hebei Province, People's Republic of China
Tel +86 18531117721
Email xuzhuoxzxz@163.com

submit your manuscript | www.dovepress.com
DovePress
http://doi.org/10.2147/CMAR.S275003

evidence has delineated that circRNAs possess powerful and complicated functions in varied cellular processes, involved in disease development, including cancer.[6,7] Numerous circRNAs were manifested to affect HCC progression by acting as oncogenic stimuli, like circMAST1, circMAN2B2 and hsa_circ_0091581;[8–10] or suppressors, such as circ-ABCB10, circRNA-0072309 and circ-0003418.[11–13] Derived from low density lipoprotein receptor (LDLR), circ_LDLR (ID: hsa_circ_0003892 in circBase; Position: chr19:11,230,767–11,238,761) was reported to be upregulated in HCC tissues in contrast to non-tumor liver tissues, evidenced by searching circRNA expression profiles, GSE94508 and GSE97332.[14] However, the role of circ_LDLR in HCC development remains to be investigated.

MicroRNAs (miRNAs) are a class of endogenous non-coding RNAs, only ~22 nucleotides long, playing vital regulatory functions in various organisms.[15] MiRNAs could affect the development and progression of multiple human diseases, including HCC.[16,17] Former literature has summarized the dual roles of miR-7 in cancers, functioning as oncogene or tumor suppressor.[18] In HCC, miR-7 was identified as an anti-tumor factor, causing HCC cell proliferation and invasion inhibition.[19] As a promising target of circ_LDLR forecasted by Circinteractome, the effects of miR-7 on circ_LDLR-mediated HCC cellular behaviors have not been illuminated.

Ring finger protein 38 (RNF38), a member of the RING ubiquitin ligase family, contains two pivotal functional motifs, implying its involvement in both protein-DNA and protein-protein interactions.[20] RNF38 was substantiated to facilitate non-small cell lung cancer,[21] gastric cancer[22] and HCC[23] progression but suppress colorectal cancer development.[24] Here, RNF38 was estimated to be a target of miR-7, while the role of circ_LDLR-mediated HCC development needs further elucidation.

In the present study, the enrichment of circ_LDLR in HCC tissues and cells was determined. Furthermore, its functional impact on malignant behaviors of HCC cells was investigated, as well as the molecular basis.

Materials and Methods

Patients and Clinical Samples

Fifty cases of HCC tissues and paired normal tissues were postoperatively acquired from Fourth Hospital of Hebei Medical University. None of them had taken a cure prior to surgery operation. All the HCC tissue samples were collected with written informed consent in accordance with the Declaration of Helsinki and with the approval of the Ethical Committee of Fourth Hospital of Hebei Medical University (IRB No.2019SJZ08).

Cell Culture and Transfection

Culture of human Liver Epithelial-2 (THLE-2, CRL-2706; American Type Culture Collection, Manassas, VA, USA), HCC cell lines Hep3B (HB-8064) and Huh7 (CL-0120; Procell, Wuhan, China) was implemented in Dulbecco's Modified Eagle Medium (HyClone, Logan, UT, USA) supplemented with 10% (v/v) fetal bovine serum (HyClone) and 1% penicillin/streptomycin (Gibco Light, Shanghai, China) at 37°C with an atmosphere of 5% CO_2/95% air.

Small interfering RNA (siRNA) specially targeting circ_LDLR (si-circ_LDLR) was introduced into Hep3B and Huh7 cells to silence circ_LDLR, with si-NC as negative control. For miR-7 overexpression or interference, miR-7 mimic (miR-7) or miR-7 inhibitor (anti-miR-7) was transfected into HCC cells, with miR-NC or anti-miR-NC as negative control. To upregulate RNF38, its overexpression vector pcDNA-RNF38 (RNF38) was introduced into HCC cells, with pcDNA as negative control. Above oligonucleotides and plasmids were all designed and synthesized by Genechem (Shanghai, China), and the transfection assay was conducted using Lipofectamine 3000 (Solarbio, Beijing, China) referring to the specifications.

Quantitative Real-Time PCR (qRT-PCR)

Total RNA derived from clinical specimens or cells was extracted using TRIzol Reagent (Beyotime, Shanghai, China), then subjected to reverse transcription into complementary DNA (cDNA) with BeyoRT™ III M-MLV reverse transcriptase (Beyotime) or TaqMan miRNA Reverse Transcription Kit (Applied Biosystems, Foster City, CA, USA). Following qPCR was carried out using SYBR Master Mix (Applied Biosystems) or miRNA-specific TaqMan MiRNA Assay Kit (Applied Biosystems). Relative expression of genes was assessed using $2^{-\Delta\Delta Ct}$ method,[25] with glyceraldehyde-3-phosphate dehydrogenase (GAPDH, for circ_LDLR, LDLR and RNF38) or U6 (for miR-7) as internal control. Sequences of qPCR primers were: circ_LDLR, 5′-AGTAGCGTGAGGGCTCTGTC-3′ (sense) and 5′-CAGCCAACAAGTTGACATCG-3′ (anti-sense); LDLR, 5′-GAATCTACTGGTCTGACCTGTCC-3′ (sense) and 5′-GGTCCAGTAGATGTTGCTGTGG-3′ (anti-sense);

miR-7, 5′-TGGAAGACTAGTGATTTTG-3′ (sense) and 5′-GAACATGTCTGCGTATCTC-3′ (anti-sense); RNF38, 5′-GGTGAGACTTCAGAGCCTGTTC-3′ (sense) and 5′-CGCTGTCTCTTAGGACTTGGAC-3′ (anti-sense); GAPDH, 5′-GTCTCCTCTGACTTCAACAGCG-3′ (sense) and 5′-ACCACCCTGTTGCTGTAGCCAA-3′ (anti-sense); U6, 5′-CTCGCTTCGGCAGCACAT-3′ (sense) and 5′-AACGCTTCACGAATTTGCGT-3′ (anti-sense).

RNase R Digestion and Actinomycin D Treatment

Both RNase R digestion and Actinomycin D treatment were applied to confirm the stability of circ_LDLR in HCC cells. For RNase R digestion assay, 10 μg total RNA derived from Hep3B and Huh7 cells was incubated with RNase R (3 U/ug; TaKaRa, Dalian, China) or not (Mock) at 37°C for 1 h. For Actinomycin D treatment assay, 2 mg/mL Actinomycin D (Amyjet, Wuhan, China) was added to medium to incubate for 0 h, 4 h, 8 h, 16 h or 24 h. After disposition with RNase R or Actinomycin D, RNA was purified and subjected for qRT-PCR assay to determine the abundance of circ_LDLR and LDLR.

Flow Cytometry

To determine cell cycle distribution, HCC cells were harvested at 24 h post-transfection, then washed and subjected to fixation with pure ethanol at 37°C overnight. Later, cells were rinsed and re-suspended in propidium iodide (PI; KeyGen, Nanjing, China) solution containing RNase A. After incubation for 1 h away from light, cell number in G0/G1, S and G2/M phases was examined using a flow cytometer (BD Biosciences, Heidelberg, Germany) with CellQuest software.

For apoptosis analysis, Annexin V-fluorescein isothiocyanate (FITC)/propidium iodide (PI) Apoptosis Detection Kit (Beyotime) was used in accordance with producer's guidance. Transfected Hep3B and Huh7 cells were collected and washed, followed by staining with Annexin V and PI at indoor temperature for 20 min in dark place. Subsequently, apoptotic cells were monitored utilizing flow cytometer.

Colony Formation Assay

At 24 h post-transfection, Hep3B and Huh7 cells (~500) were plated on 6-well plates and routinely cultured for 2 weeks. Afterwards, generated colonies (exceeding 50 cells) were immobilized with methanol, dyed with crystal violet (Beyotime), photographed and counted under a microscope with Image J software. Colony formation rate = Number of generated colonies/Number of seeded cells × 100%.

Methyl Thiazolyl Tetrazolium (MTT) Assay

After transfection, Hep3B and Huh7 cells (5×10^3) were seeded into 96-well plates. At indicated time points (0 d, 1 d, 2 d and 3 d), 10 μL MTT reagent (0.5 mg/mL; Beyotime) was pipetted into each well. After incubation for additional 4 h, dimethyl sulfoxide (DMSO; Solarbio) was added to terminate reaction. Later, cell viability was assessed by the absorbance at 570 nm using a Microplate Reader (Bio-Rad Laboratories, Inc., Hercules, CA, USA).

Western Blot Assay

Clinical specimens or cells were lysed in Radioimmunoprecipitation Assay (RIPA) buffer (Beyotime) supplemented with proteinase and phosphatase inhibitors. Following quantification, 40 μg protein samples were loaded on 10% sodium dodecyl sulfate polyacrylamide gel electrophoresis (SDS-PAGE) and transferred onto polyvinylidene fluoride membranes (Bio-Rad Laboratories, Inc.). The membranes were subjected to blockage with 5% skim milk for 2 h, incubation with primary antibody against Ki67 (sc-23,900; Santa Cruz Biotechnology, Santa Cruz, CA, USA) E-cadherin (sc-8426; Santa Cruz Biotechnology), N-cadherin (sc-8424; Santa Cruz Biotechnology), vimentin (sc-6260; Santa Cruz Biotechnology), RNF38 (sc-515,213; Santa Cruz Biotechnology) or GAPDH (sc-47,724; Santa Cruz Biotechnology) at 4°C overnight and interaction with secondary antibody (sc-516,102; Santa Cruz Biotechnology) for 2 h. At last, protein blots were visualized using a chemiluminescence kit (Santa Cruz Biotechnology).

Transwell Assay

Transwell chamber (8 μm size; BD Biosciences, San Jose, CA, USA) enveloped with or without Matrigel (BD Biosciences) was used for cell invasion or migration detection, respectively. After transfection, Hep3B and Huh7 cells re-suspended in serum-free medium were plated onto the upper chambers. While, complete medium was placed into the lower ones. At 48 h post-incubation, cells invaded or migrated through the polycarbonic membrane were fixed in methanol, dyed with crystal violet, photographed and counted under a microscope (100 ×).

Dual-Luciferase Reporter Assay

Bioinformatic analysis for the molecular target genes of circ_LDLR and miR-7 was conducted by feat of Circinteractome (https://circinteractome.nia.nih.gov) and Starbase 3.0 (http://starbase.sysu.edu.cn/index.php). Wide-type luciferase reporters (circ_LDLR-wt and RNF38-wt) were constructed by inserting partial sequences of circ_LDLR or RNF38 3′UTR into psiCHECK-2 luciferase reporter vector (Promega, Southampton, UK). After mutating complementary sites using Quick Change Site-Directed Mutagenesis kit (Agilent, Santa Clara, CA, USA), mutant-type luciferase reporters (circ_LDLR-mut and RNF38-mut) were established. Afterwards, each luciferase reporter and miR-NC or miR-7 were co-transfected into Hep3B and Huh7 cells, followed by determination of luciferase density using Dual-Luciferase Reporter Assay System (Promega) based on recommended instructions.

Xenograft Assay in Nude Mice

Prior to conduct experiments in nude mice, we got approval from the Ethics Committee of Fourth Hospital of Hebei Medical University. Animal studies were performed in compliance with the ARRIVE guidelines and the Basel Declaration. All animals received humane care according to the National Institutes of Health (USA) guidelines. Small hairpin RNA (shRNA) targeting circ_LDLR (sh-circ_LDLR; Genechem) was stably introduced into Hep3B cells, with sh-NC (Genechem) as negative control. Five weeks old nude mice purchased from Beijing Laboratory Animal Center (Beijing, China) were subcutaneously injected with 5×10^6 Hep3B cells stably expressing sh-NC or sh-circ_LDLR (n=5). 7 d later, the size of formed tumors was recorded every 5 d and computed using the formula: volume= $0.5 \times$ width^2 × length. 35 d after injection, all mice were killed, and tumors were resected for weigh. Afterwards, abundance of circ_LDLR, miR-7 and RNF38 was examined.

Statistical Analysis

All experiments in this project were independently carried out for at least 3 times. Data were processed utilizing SPSS 20.0 statistical software (SPSS, Chicago, IL, USA) and exhibited as mean ± standard deviation. For difference analysis, Student's *t*-test or one-way analysis of variance was applied. Pearson correlation analysis was hired to determine the correlation among expression of circ_LDLR, miR-7 and RNF38 in 50 cases of HCC tissues. What's more, a *P* value less than 0.05 was defined to be statistically significant.

Results

Circ_LDLR Was Obviously Upregulated in HCC Tissues and Cells

At first, the expression of circ_LDLR in HCC tissues and matched normal tissues were detected by qRT-PCR assay, the results revealed that circ_LDLR was upregulated in HCC tissues relative to normal tissues (Figure 1A). Additionally, the upregulation of circ_LDLR was also detected in Hep3B and Huh7 cells, when compared with THLE-2 cells (Figure 1B). After digestion with RNase R, relative expression of LDLR, rather than circ_LDLR was significantly cut down in HCC cells (Figure 1C and D). Furthermore, circ_LDLR had a longer half-life in contrast to linear LDLR in Hep3B and Huh7 cells treated with actinomycin D (Figure 1E and F). Collectively, circ_LDLR was highly expressed in HCC tissues and cells, with loop structure.

Depletion of circ_LDLR Inhibited HCC Cell Proliferation and Metastasis

Having known that circ_LDLR was obviously upregulated in HCC tissues and cells, we then conducted loss-of-function assays to investigate its role in HCC development. Si-circ_LDLR was introduced into Hep3B and Huh7 cells to silence circ_LDLR, the knockdown efficiency was exhibited in Figure 2A and B. But the LDLR expression was unchanged. Obviously, our data showed that circ_LDLR knockdown decreased HCC cells in S phase, while increased cells in G0/G1 phase (Figure 2C and D). Circ_LDLR knockdown also reduced the colony formation ability (Figure 2E) and cell viability (Figure 2F and G) of HCC cells, as demonstrated by colony formation and MTT assays. Results of Western blot assay manifested that circ_LDLR knockdown triggered the downregulation of Ki67 in HCC cells (Figure 2H). As shown in Figure 2I–L, depletion of circ_LDLR efficiently repressed HCC cell metastasis, reflected by the declined number of migrated and invaded cells, upregulation of E-cadherin and downregulation of N-cadherin vimentin. Moreover, more apoptotic Hep3B and Huh7 cells were observed in si-circ_LDLR group (Figure 2M). Taken together, circ_LDLR knockdown suppressed proliferation and metastasis of HCC cells.

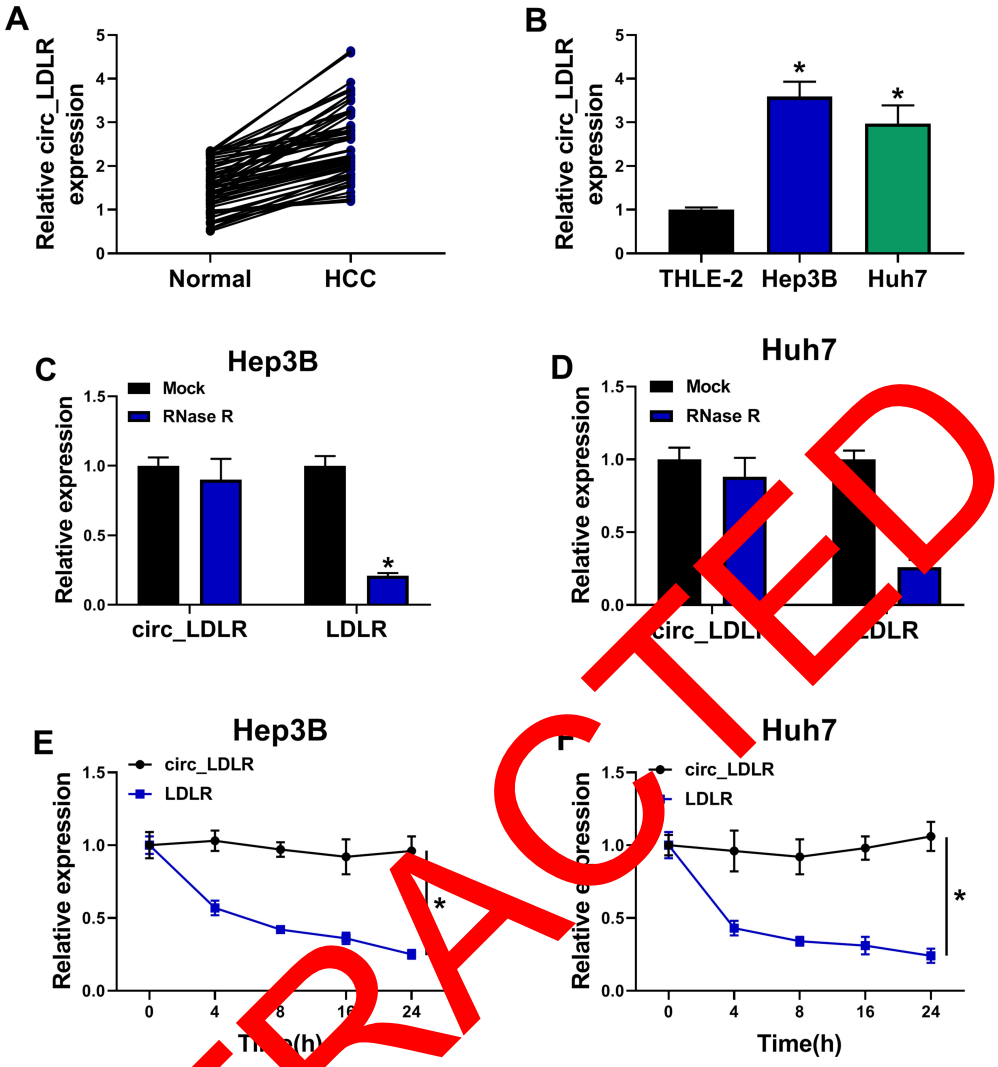

Figure 1 Circ_LDLR was obviously upregulated and featured with loop structure. (**A**) QRT-PCR assay for the relative expression of circ_LDLR in HCC tissues and adjacent normal tissues (n=50). (**B**) QRT-PCR assay for the relative expression of circ_LDLR in THLE-2, Hep3B and Huh7 cells. (**C, D**) QRT-PCR assay for the relative expression of circ_LDLR and LDLR in RNA isolated from Hep3B and Huh7 cells digested with RNase R or not (Mock). (**E, F**) QRT-PCR assay for the relative expression of circ_LDLR in Hep3B and Huh7 cells disposed with Actinomycin D at indicated time points. *$P < 0.05$.

Circ_LDLR Could Sponge miR-7 in HCC Cells

To explore the possible mechanism by which circ_LDLR impacting the cellular behaviors of HCC cells, the miRNAs directly interacted with circ_LDLR were estimated via Circinteractome. And miR-7 was identified to be a candidate, the binding sites between circ_LDLR and miR-7 were exhibited in Figure 3A. Following dual-luciferase reporter assay was performed to validate the potential relationship. Apparently, luciferase density in Hep3B and Huh7 cells co-transfected with circ_LDLR-wt and miR-7 was lower than that in cells co-transfected with circ_LDLR-wt and miR-NC; But, luciferase activity in cells co-transfected with circ_LDLR-mut and miR-NC or miR-7 was changeless (Figure 3B and C), indicating direct binding of circ_LDLR and miR-7. Moreover, miR-7 expression was upregulated by circ_LDLR knockdown (Figure 3D). Then, expression of miR-7 in HCC tissues and cells was examined by qRT-PCR assay. As depicted in Figure 3E and G, miR-7 expression was significantly declined in HCC tissues and cells in comparison to corresponding control. We also found that miR-7 expression was inversely correlated with that of circ_LDLR in HCC tissues (Figure 3F). These data suggested that circ_LDLR acted as sponge of miR-7 in HCC cells.

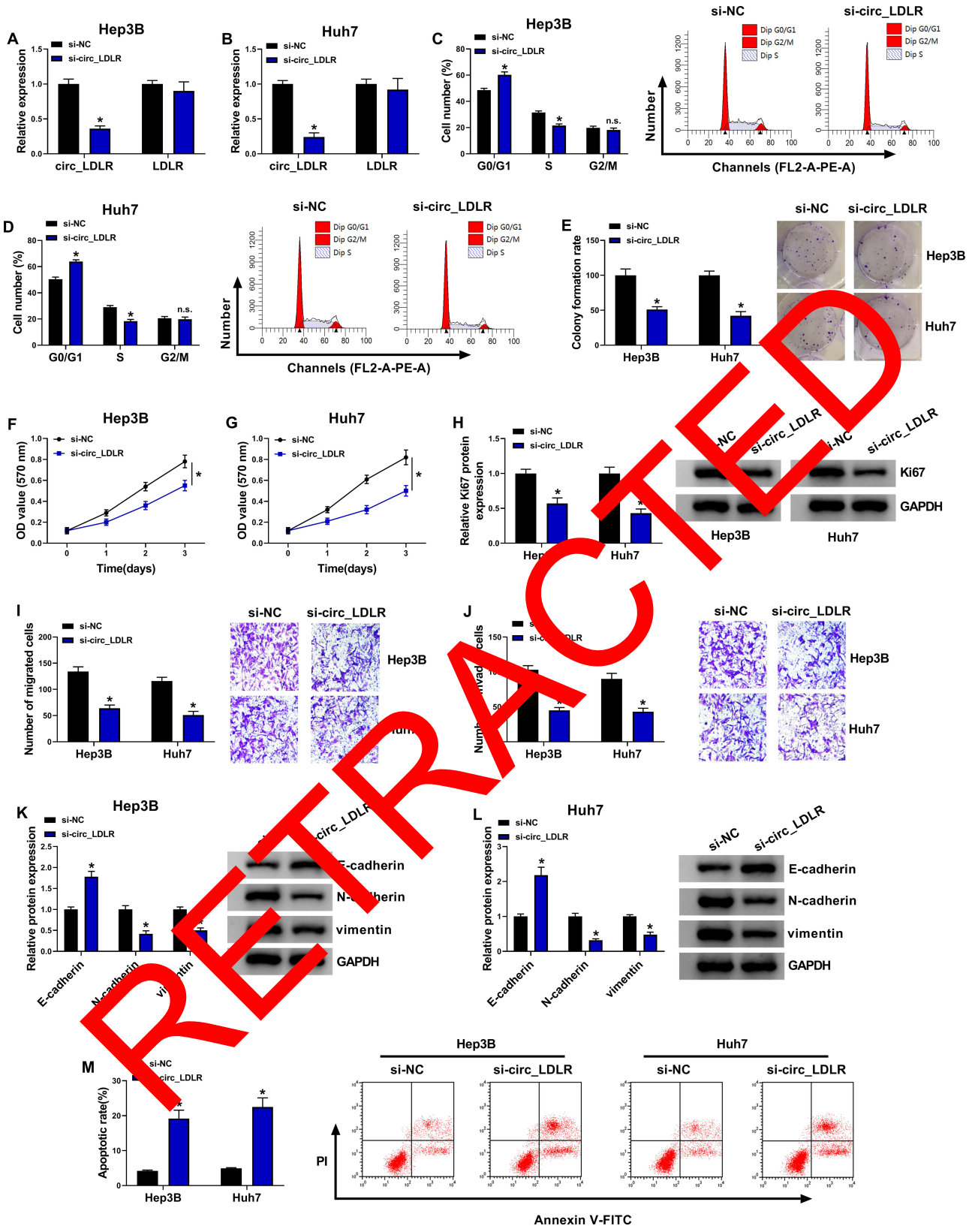

Figure 2 Depletion of circ_LDLR inhibited HCC cell proliferation and metastasis. Hep3B and Huh7 cells were transfected with si-NC or si-circ_LDLR. (**A, B**) QRT-PCR assay for the relative expression of circ_LDLR and LDLR in transfected cells. (**C, D**) Flow cytometry for distribution of transfected cells in G0/G1, S and G2/M phases. (**E**) Colony formation assay for the colony formation ability of transfected cells. (**F, G**) MTT assay for the cell viability of transfected cells. (**H**) Western blot assay for the protein level of Ki67 in transfected cells. (**I, J**) Transwell assay for number of migrated and invaded cells in transfected cells. (**K, L**) Western blot assay for the protein levels of E-cadherin N-cadherin and vimentin in transfected cells. (**M**) Flow cytometry for apoptotic cells in transfected cells. *$P < 0.05$.

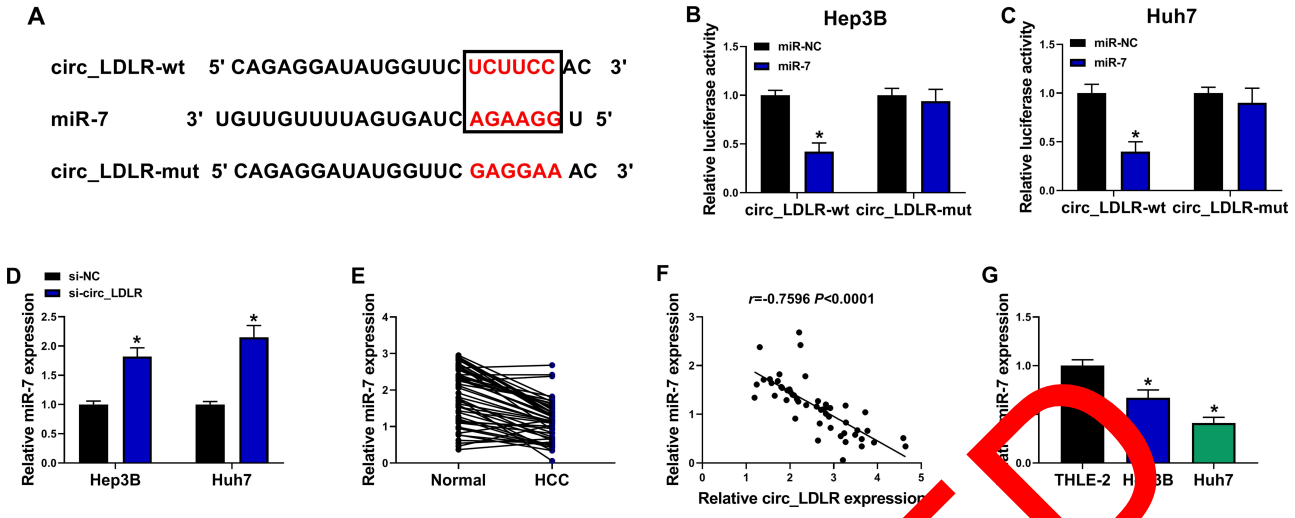

Figure 3 Circ_LDLR could sponge miR-7 in HCC cells. (**A**) The binding sites between circ_LDLR and miR-7 predicted by Circinteractome. (**B**, **C**) Dual-luciferase reporter assay for the luciferase activity in cells co-transfected with circ_LDLR-wt or circ_LDLR-mut and miR-NC or miR-7. (**D**) QRT-PCR assay for the relative expression of miR-7 in Hep3B and Huh7 cells transfected with si-NC or si-circ_LDLR. (**E**) QRT-PCR assay for the relative expression of miR-7 in HCC tissues and adjacent normal tissues (n=50). (**F**) Pearson correlation analysis for the correlation between the expression of circ_LDLR and miR-7 in 50 cases of HCC tissues (r=−0.7596, P < 0.0001). (**G**) QRT-PCR assay for the relative expression of miR-7 in THLE-2, Hep3B and Huh7 cells. *P < 0.05.

Interference of miR-7 Almost Reversed the circ_LDLR Knockdown-Induced Inhibition of HCC Cell Proliferation and Metastasis

Given the targeting relationship between circ_LDLR and miR-7, the functional effects of the two on the HCC progression were investigated. QRT-PCR assay showed that circ_LDLR knockdown apparently increased the level of miR-7 in Hep3B and Huh7 cells, but miR-7 inhibitor reduced this upregulation effect (Figure 4A). Following rescue experiments uncovered that the circ_LDLR knockdown-induced declined HCC cells in S phase (Figure 4B and C), colony formation ability (Figure 4D) and cell viability (Figure 4E and F), downregulation of Ki67 (Figure 4G), HCC cell metastasis inhibition (Figure 4H–J), as well as elevated apoptotic rate (Figure 4L) in HCC cells were largely relieved by miR-7 inhibitor. These data indicated that interference of miR-7 could reverse the tumor suppressor role of circ_LDLR knockdown in HCC cell proliferation and metastasis.

RNF38 Was a Direct Binding Target of miR-7 in HCC Cells

Through predicting target of miRNA by Starbase3.0, 3′-UTR of RNF38 was considered as a putative target of miR-7, the binding position is shown in Figure 5A. Furthermore, dual-luciferase reporter assay revealed that luciferase activity was obviously lower in Hep3B and Huh7 cells co-transfected with RNF38-wt and miR-than that in cells co-transfected with RNF38-wt and miR-NC (Figure 5B and C), suggesting that RNF38 was a direct target of miR-7. We further examined the impact of miR-7 on RNF38 expression in HCC cells. The overexpression efficiency of miR-7 mimic and the interference efficiency of miR-7 inhibitor in HCC cells were exhibited in Figure 5D, which were determined by qRT-PCR assay. Moreover, we found that miR-7 overexpression efficiently decreased mRNA and protein expression levels of RNF38 in Hep3B and Huh7 cells, while miR-7 inhibitor triggered reverse results (Figure 5E and F). As exhibited in Figure 5G, RNF38 mRNA expression was increased in HCC tissues versus adjacent normal tissues. Pearson correlation analysis disclosed a negative correlation between expression of RNF38 mRNA and miR-7 (Figure 5H), and a positive correlation between the expression of RNF38 mRNA and circ_LDLR (Figure 5I) in HCC tissues. As expected, RNF38 protein expression was upregulated in HCC tissues in comparison with matched normal tissues (Figure 5J). Also, RNF38 expression was upregulated in Hep3B and Huh7 cells relative to THLE-2 cells, at mRNA (Figure 5K) and protein (Figure 5L) levels. Moreover, we found that miR-7 inhibitor reversed the circ_LDLR knockdown-mediated downregulation of RNF38 in HCC cells (Figure 5M and N). Above results implied that RNF38 was a direct target of miR-7 in HCC cells.

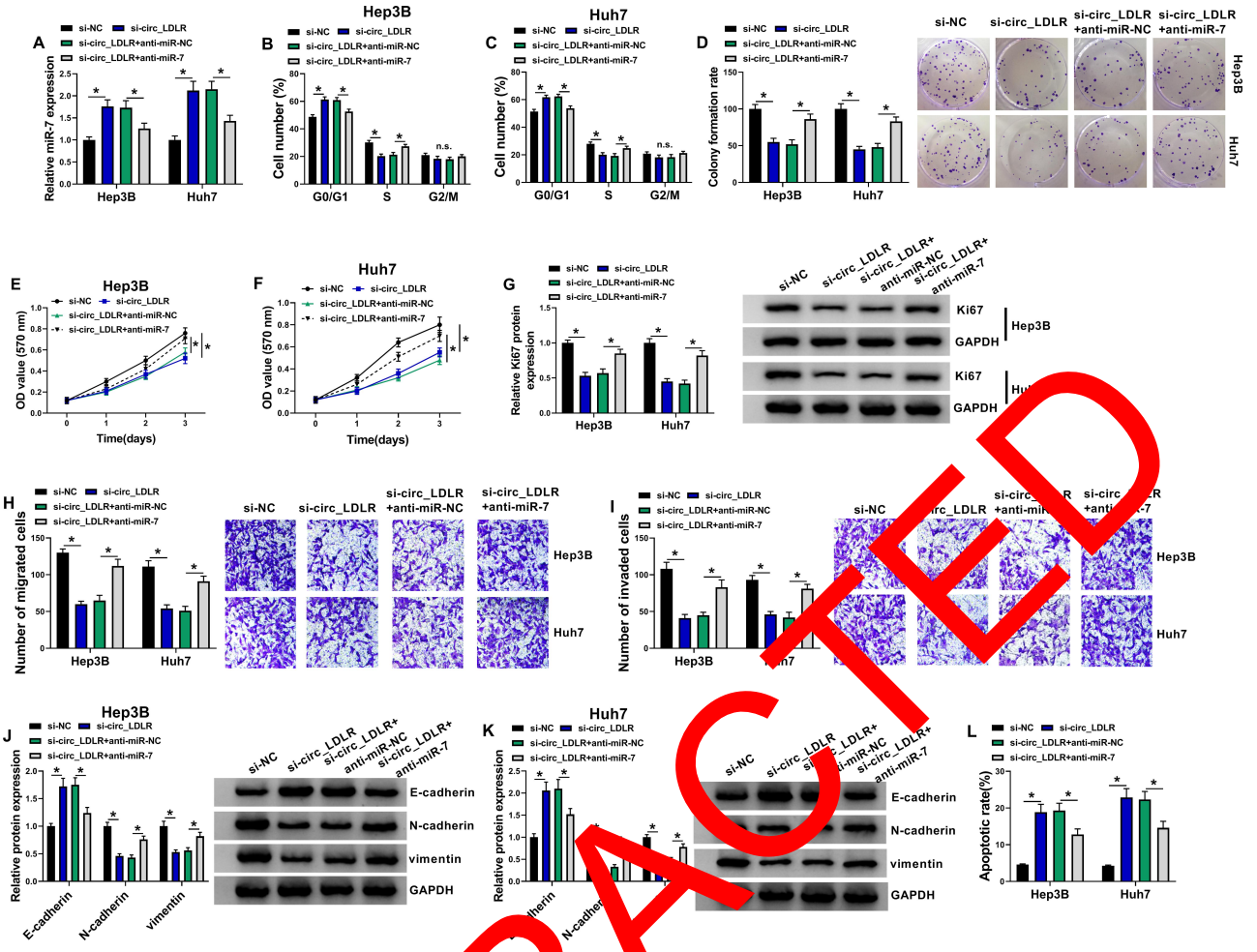

Figure 4 Interference of miR-7 almost reversed the circ_LDLR knockdown-induced inhibition of HCC cell proliferation and metastasis. Hep3B and Huh7 cells were transfected with si-NC, si-circ_LDLR, si-circ_LDLR+anti-miR-NC or si-circ_LDLR+anti-miR-7. (**A**) QRT-PCR assay for the relative expression of miR-7 in transfected cells. (**B, C**) Flow cytometry for distribution of transfected cells in G0/G1 and G2/M phases. (**D**) Colony formation assay for the colony formation ability of transfected cells. (**E, F**) MTT assay for the cell viability of transfected cells. (**G**) Western blot assay for the protein level of Ki67 in transfected cells. (**H, I**) Transwell assay for number of migrated and invaded cells in transfected cells. (**J, K**) Western blot assay for the protein levels of E-cadherin N-cadherin and vimentin in transfected cells. (**L**) Flow cytometry for apoptotic cells in transfected cells. *$P < 0.05$

miR-7 Repressed HCC Cell Proliferation and Metastasis by Targeting RNF38

Next, the co-effects of miR-7 and RNF38 on HCC progression were explored. As shown in Figure 6A and B, RNF38 overexpression weakened miR-7-induced downregulation of RNF38 in Hep3B and Huh7 cells. What's more, miR-7 resulted in lessened HCC cells in S phase (Figure 6C and D), colony formation ability (Figure 6E) and cell viability (Figure 6F and G), downregulation of Ki67 (Figure 6H), repressed HCC cell metastasis (Figure 6I–L), as well as raised apoptotic rate (Figure 6M) in HCC cells, which were all ameliorated by additional RNF38. Therefore, miR-7 repressed HCC cell proliferation and metastasis by targeting RNF38.

Knockdown of circ_LDLR Suppressed Tumorigenesis in HCC Xenografts in vivo

Animal experiments in vivo were performed to further explore the role of circ_LDLR in HCC progression. Hep3B cells stably expressing sh-NC or sh-circ_LDLR were inoculated into nude mice to establish xenograft tumor model. Compared to sh-NC, circ_LDLR knockdown efficiently blocked the size (Figure 7A, Supplementary Figure 1) and weight (Figure 7B) of HCC tumors. In addition, circ_LDLR (Figure 7C) and RNF38 (Figure 7E and F) were downregulated, while miR-7 (Figure 7D) was upregulated in generated tumors of sh-circ_LDLR group versus sh-NC group. Moreover, circ_LDLR depletion hampered EMT process in vivo. Thus, we concluded that circ_LDLR knockdown suppressed tumor growth in vivo.

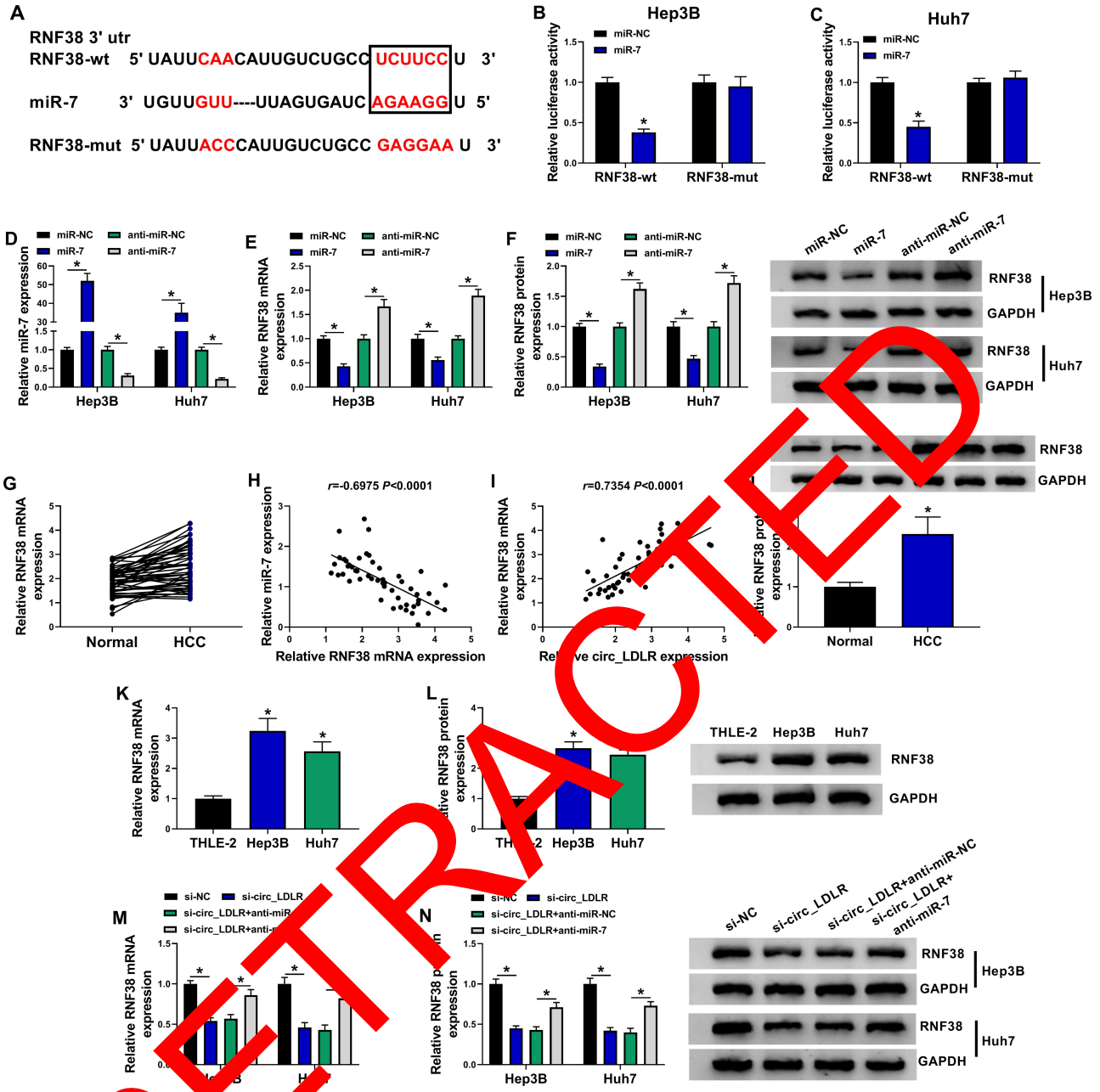

Figure 5 RNF38 was a direct binding target of miR-7 in HCC cells. (**A**) The binding sites between miR-7 and RNF38 forecasted by Starbase3.0. (**B, C**) Dual-luciferase reporter assay for the luciferase activity in cells co-transfected with RNF38-wt or RNF38-mut and miR-NC or miR-7. (**D**) QRT-PCR assay for the relative expression of miR-7 in Hep3B and Huh7 cells transfected with miR-7, anti-miR-NC or anti-miR-7. (**E, F**) QRT-PCR and Western blot assays for the mRNA (**E**) and protein (**F**) expression levels of RNF38 in Hep3B and Huh7 cells transfected with miR-NC, miR-7, anti-miR-NC or anti-miR-7. (**G**) QRT-PCR assay for the mRNA expression level of RNF38 in HCC tissues and adjacent normal tissues (n=50). (**H**) Pearson correlation analysis for the correlation between the expression of RNF38 mRNA and miR-7 in 50 cases of HCC tissues (r=−0.6975, P < 0.0001). (**I**) Pearson correlation analysis for the correlation between the expression of RNF38 mRNA and circ_LDLR in 50 cases of HCC tissues (r=0.7354, P < 0.0001). (**J**) Western blot assay for the protein expression level of RNF38 in HCC tissues and adjacent normal tissues. (**K, L**) QRT-PCR and Western blot assays for the mRNA (**K**) and protein (**L**) expression levels of RNF38 in THLE-2, Hep3B and Huh7 cells. (**M, N**) QRT-PCR and Western blot assays for the mRNA (**M**) and protein (**N**) expression levels of RNF38 in Hep3B and Huh7 cells transfected with si-NC, si-circ_LDLR, si-circ_LDLR+anti-miR-NC or si-circ_LDLR+anti-miR-7. *P < 0.05.

Discussion

There exists a well-established fact that circRNAs are closely associated with the pathogenesis of HCC, and serve as diagnostic biomarkers and therapeutic targets.[26] In this project, the dysregulation of circ_LDLR was detected in HCC tissues and cells; its promoted role in HCC cell proliferation, metastasis and tumorigenicity was elucidated, as well as the regulatory axis, circ_LDLR/miR-7/RNF38, in HCC progression.

Through overlapping two circRNA expression profiles (GSE94508 and GSE97332), Qiu et al observed the

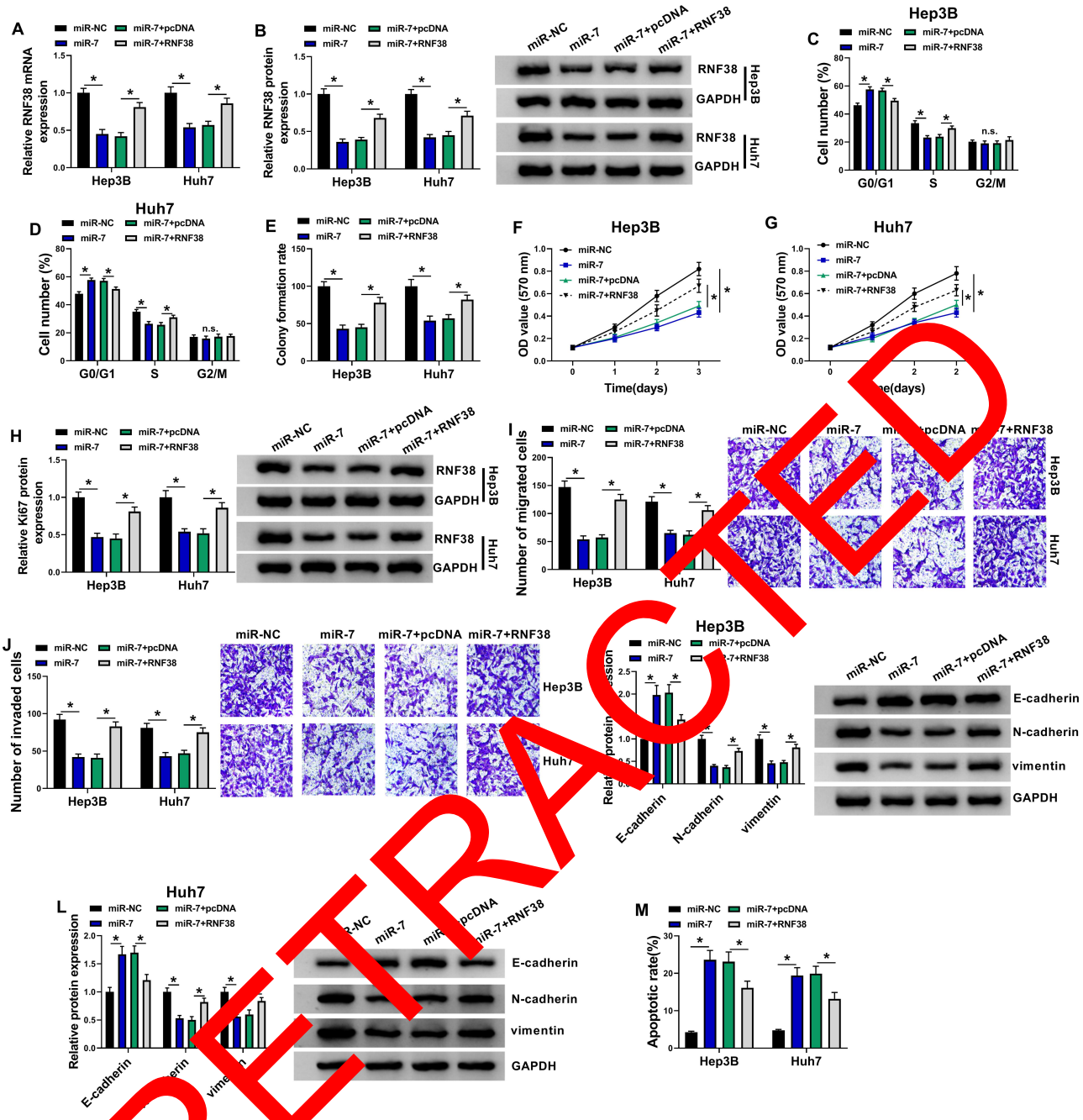

Figure 6 MiR-7 suppressed Huh7 cell proliferation and metastasis by targeting RNF38. Hep3B and Huh7 cells were transfected with miR-NC, miR-7, miR-7+pcDNA or miR-7+RNF38. (**A, B**) qRT-PCR and Western blot assays for the mRNA and protein expression levels of RNF38 in transfected cells. (**C, D**) Flow cytometry for distribution of transfected cells in G0/G1, S and G2/M phases. (**E**) Colony formation assay for the colony formation ability of transfected cells. (**F, G**) MTT assay for the cell viability of transfected cells. (**H**) Western blot assay for the protein level of Ki67 in transfected cells. (**I, J**) Transwell assay for number of migrated and invaded cells in transfected cells. (**K, L**) Western blot assay for the protein levels of E-cadherin, N-cadherin and vimentin in transfected cells. (**M**) Flow cytometry for apoptotic cells in transfected cells. *P < 0.05.

upregulation of circ_LDLR (hsa_circ_0003892 in circBase) in HCC tissues when compared to healthy tissues.[14] From our data, circ_LDLR was upregulated in HCC tissues and cells. Besides, depletion of circ_LDLR was substantiated to repress proliferation and metastasis of HCC cells in vitro, as well as tumor growth in vivo, suggesting the oncogenic role of circ_LDLR in HCC.

Mechanically, circRNAs could exert their own roles by serving as ceRNAs, so as to regulate HCC development.[27] Here, miR-7 was predicted to be a target of circ_LDLR,

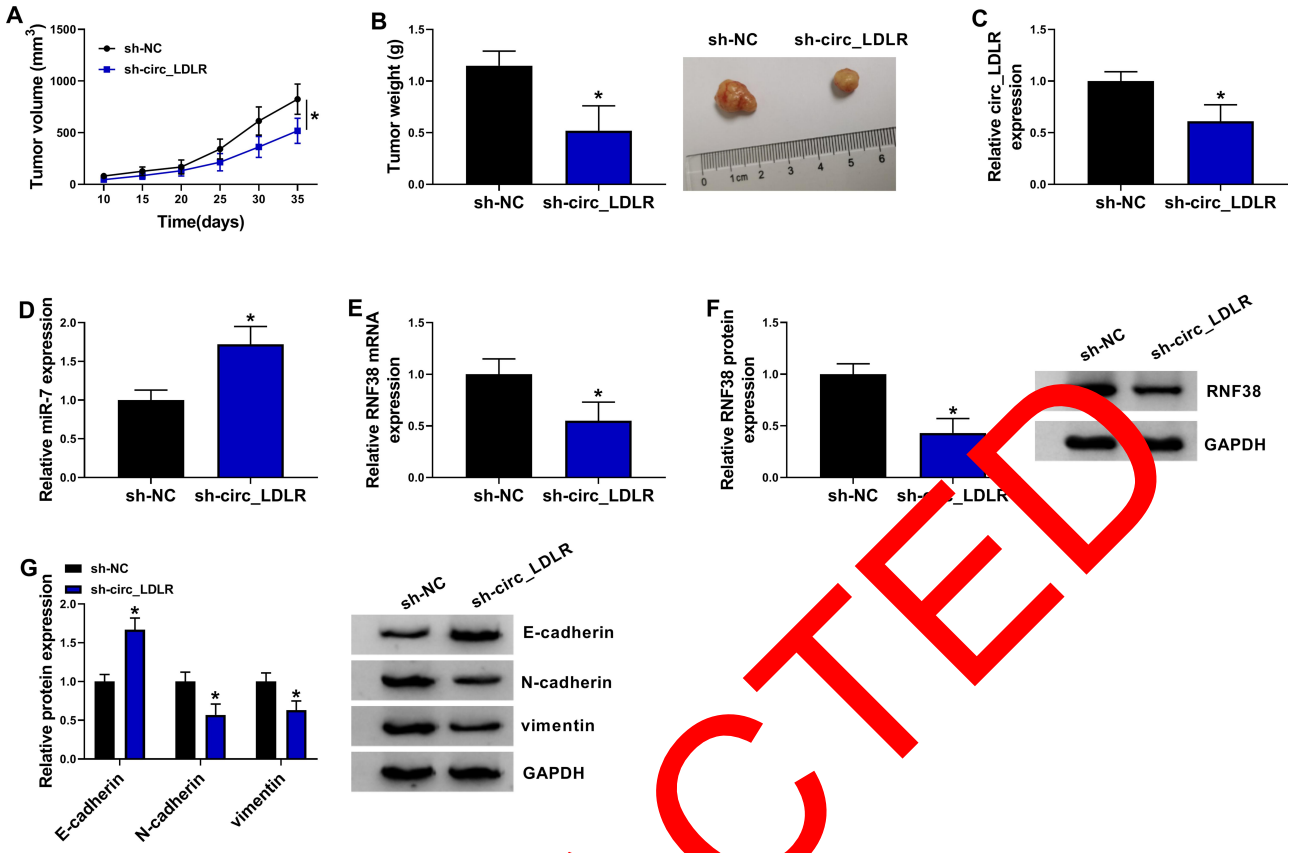

Figure 7 Knockdown of circ_LDLR suppressed tumorigenesis in HCC xe[illegible] vivo. Nude mice were implanted with Hep3B cells stably expressing sh-NC or sh-circ _LDLR. (**A**) Volume of xenograft tumor. (**B**) Weight and picture of xenograft tumor. (**C**) QRT-PCR assay for the expression of circ_LDLR (**C**) and miR-7 (**D**) in xenograft tumor. (**E, F**) QRT-PCR and Western blot assays for the mRNA (**E**) and protein (**F**) expression levels of RNF38 in xenograft tumor. (**G**) Western blot assay for the protein levels of E-cadherin, N-cadherin and vimentin in xenograft tumor. $^{*}P < 0.05$.

which was testified by dual-luciferase reporter assay. MiR-7, 23-nucleotide long, possesses dual roles in cancer progression; Also, miR-7 could act as prognostic biomarker and therapeutic target of certain malignancies.[28] Moreover, miR-7 was sponged by several circRNAs to participate in tumor progression.[29–31] In this project, we found that interference of miR-7 could attenuate circ_LDLR knockdown-induced inhibitory impact on HCC cell proliferation and metastasis. In other words, circ_LDLR performed oncogenic role in HCC by sponging miR-7.

Previous researches corroborated that miR-7 could inhibit HCC progression by targeting KLF-4,[19] PIK3CD, mTOR, and p70S6K[32] or CCNE1.[33] Likewise, the anti-HCC activity of miR-7 was also detected in our study. Subsequently, Starbase3.0 was utilized to search the downstream target gene of miR-7, and RNF38 was identified as a candidate, which was then confirmed by dual-luciferase reporter assay.

Currently, only a few reports described the functional role of RNF38 in human malignancies. In non-small cell lung cancer, RNF38 could induce proliferation and metastasis of tumor cells.[21] And RNF38 was a poor prognosis indicator of gastric cancer patients, and could contribute to cell growth.[22] Inversely, RNF38 upregulation hindered growth of colorectal cancer cells by destabilizing LDB1.[24] RNF38 was upregulated in HCC, and introduction of RNF38 conferred HCC cell mobility and proliferation by activating TGF-β signaling.[23] In the present study, we also detected upregulation of RNF38 in HCC tissues and cells; and enforced expression of RNF38 largely relieved miR-7-induced inhibited HCC proliferation and metastasis, suggesting the involvement of RNF38 in circ_LDLR/miR-7/RNF38 axis in HCC progression.

In conclusion, circ_LDLR was up-regulated in HCC tissues and cells. Additionally, we were the first to validate that circ_LDLR exerted its oncogenic role in HCC, at least partly, by modulating miR-7/RNF38 axis. Our findings afforded a promising treatment target of HCC.

Funding

There is no funding to report.

Disclosure

The authors declare that they have no financial or non-financial conflicts of interest for this work.

References

1. Dimitroulis D, Damaskos C, Valsami S, et al. From diagnosis to treatment of hepatocellular carcinoma: an epidemic problem for both developed and developing world. *World J Gastroenterol*. 2017;23(29):5282–5294. doi:10.3748/wjg.v23.i29.5282
2. Intaraprasong P, Siramolpiwat S, Vilaichone RK. Advances in management of hepatocellular carcinoma. *Asian Pac J Cancer Prev*. 2016;17(8):3697–3703.
3. Sohal DP, Sun W. Hepatocellular carcinoma: prevention and therapy. *Curr Oncol Rep*. 2011;13(3):186–194. doi:10.1007/s11912-011-0165-0
4. Bruix J, Gores GJ, Mazzaferro V. Hepatocellular carcinoma: clinical frontiers and perspectives. *Gut*. 2014;63(5):844–855. doi:10.1136/gutjnl-2013-306627
5. Jeck WR, Sorrentino JA, Wang K, et al. Circular RNAs are abundant, conserved, and associated with ALU repeats. *Rna*. 2013;19(2):141–157. doi:10.1261/rna.035667.112
6. Liu J, Liu T, Wang X, He A. Circles reshaping the RNA world: from waste to treasure. *Mol Cancer*. 2017;16(1):58. doi:10.1186/s12943-017-0630-y
7. Cortés-López M, Miura P. Emerging functions of circular RNAs. *Yale J Biol Med*. 2016;89(4):527–537.
8. Yu X, Sheng P, Sun J, et al. The circular RNA circMAST1 promotes hepatocellular carcinoma cell proliferation and migration by sponging miR-1299 and regulating CTNND1 expression. *Cell Death Dis*. 2020;11(5):340. doi:10.1038/s41419-020-2532-y
9. Fu X, Zhang J, He X, et al. Circular RNA MAPKAPK2 promotes cell proliferation of hepatocellular carcinoma cells via the miRNA-217/MAPK1 axis. *J Cancer*. 2020;11(11):3318–3326. doi:10.7150/jca.36500
10. Wei X, Zheng W, Tian P, et al. Oncogenic hsa_circ_0091[illegible]1 promotes the malignancy of HCC cell through binding miR-526b from degrading c-MYC mRNA. *Cell Cycle*. 2020;19(7):817–824. doi:10.1080/15384101.2020.1731945
11. Yang W, Ju HY, Tian [illegible] Circular RNA-ABCB10 suppresses hepatocellular carcinoma progression through upregulating NRP1/ABL2 via sponging miR-[illegible]-5p/miR-[illegible]52-5p. *Eur Rev Med Pharmacol Sci*. 2020;24(5):23[illegible]–235[illegible] doi:10.2[illegible]55/e[illegible]ev_202003_20501
12. Yu Q, Dai [illegible]shu M. Circular RNA [illegible]2309 has antitumor influences in Hep3B cell line [illegible]ing microRNA-665. *Biofactors*. 2020. doi:10.1002/[illegible]18
13. Chen H, Liu S, [illegible]M, Huang P, Li X. circ_0003418 inhibits tumorigenesis and cisplatin chemoresistance through Wnt/β-catenin pathway in hepatocellular carcinoma. *Onco Targets Ther*. 2019;12:9539–9549. doi:10.2147/ott.s229507
14. Qiu L, Wang T, Ge Q, et al. Circular RNA signature in hepatocellular carcinoma. *J Cancer*. 2019;10(15):3361–3372. doi:10.7150/jca.31243
15. Cai Y, Yu X, Hu S, Yu J. A brief review on the mechanisms of miRNA regulation. *Genomics Proteomics Bioinformatics*. 2009;7(4):147–154. doi:10.1016/s1672-0229(08)60044-3
16. Vishnoi A, Rani S. MiRNA biogenesis and regulation of diseases: an overview. *Methods Mol Biol*. 2017;1509:1–10. doi:10.1007/978-1-4939-6524-3_1
17. Li D, Zhang J, Li J. Role of miRNA sponges in hepatocellular carcinoma. *Clin Chim Acta*. 2020;500:10–19. doi:10.1016/j.cca.2019.09.013
18. Gu DN, Huang Q, Tian L. The molecular mechanisms and therapeutic potential of microRNA-7 in cancer. *Expert Opin Ther Targets*. 2015;19(3):415–426. doi:10.1517/14728222.2014.988708
19. Wu W, Liu S, Liang Y, Zhou Z, Liu X. MiR-7 inhibits progression of hepatocarcinoma by targeting KLF-4 and promises a novel diagnostic biomarker. *Cancer Cell Int*. 2017;17(1):31. doi:10.1186/s12935-017-0386-x
20. Eisenberg I, Hochner H, Levi T, Yelin R, Kahan T, Mitrani-Rosenbaum S. Cloning and characterization of a novel human gene RNF38 encoding a conserved putative protein with a RING finger domain. *Biochem Biophys Res Commun*. 2002;294(5):1169–1176. doi:10.1016/s0006-291x(02)005843
21. Xiong D, Zhu S-Q, Wu Y-B, et al. Ri[illegible] finger pro[illegible]n 38 promote non-small cell lung cancer progre[illegible]on by endow[illegible] cell EMT phenotype. *J Cancer*. 2018;9(5):841–8[illegible] doi:10.7150/[illegible].23138
22. Zhang J, Wu H, Yi B, et al. RING finger [illegible]otein 38 i[illegible]uces gastric cancer cell growth by decr[illegible]ing the stability [illegible]f th[illegible]rotein tyrosine phosphatase SHP−1. *FEBS [illegible]t*. 2018;[illegible]2(18):3092–3100. doi:10.1002/1873-3468.13[illegible]5
23. Peng R, Zhang P[illegible], Yang X[illegible]al. Overe[illegible]ression of RNF38 facilitates TGF-β s[illegible]ling by ubiqu[illegible]nati[illegible]and degrading AHNAK in hepatocellu[illegible] carc[illegible]oma. *J Exp C[illegible] Cancer Res*. 2019;38(1):113. doi:10.1186/s13046-0[illegible]1113-3
24. Huan[illegible]ang P, Ge H, [illegible]l. RING finger protein 38 mediates LIM domain binding 1 degradation and regulates cell growth in colorectal cancer. *Onco Targets Ther*. 2020;13:371–379. doi:10.2147/ott.s[illegible]4828
25. Li[illegible] KJ, Schmi[illegible]gen TD. Analysis of relative gene expression data using [illegible]l-time quantitative PCR and the 2−ΔΔCT method. *Methods*. 2001;25(4):402–408. doi:10.1006/meth.2001.1262
26. [illegible]i P, Song Y, et al. Progress and prospects of circular RNAs in hepatocellular carcinoma: novel insights into their function. *J Cell Physiol*. 2018;233(6):4408–4422. doi:10.1002/jcp.26154
27. Fu L, Jiang Z, Li T, Hu Y, Guo J. Circular RNAs in hepatocellular carcinoma: functions and implications. *Cancer Med*. 2018;7(7):3101–3109. doi:10.1002/cam4.1574
28. Horsham JL, Kalinowski FC, Epis MR, Ganda C, Brown RA, Leedman PJ. Clinical potential of microRNA-7 in cancer. *J Clin Med*. 2015;4(9):1668–1687. doi:10.3390/jcm4091668
29. Li H, Lan M, Liao X, Tang Z, Yang C. Circular RNA cir-ITCH promotes osteosarcoma migration and invasion through cir-ITCH/miR-7/EGFR pathway. *Technol Cancer Res Treat*. 2020;19:1533033819898728. doi:10.1177/1533033819898728
30. Wang Q, Li Z, Hu Y, et al. Circ-TFCP2L1 promotes the proliferation and migration of triple negative breast cancer through sponging miR-7 by inhibiting PAK1. *J Mammary Gland Biol Neoplasia*. 2019;24(4):323–331. doi:10.1007/s10911-019-09440-4
31. Liu L, Liu FB, Huang M, et al. Circular RNA ciRS-7 promotes the proliferation and metastasis of pancreatic cancer by regulating miR-7-mediated EGFR/STAT3 signaling pathway. *Hepatobiliary Pancreat Dis Int*. 2019;18(6):580–586. doi:10.1016/j.hbpd.2019.03.003
32. Fang Y, Xue JL, Shen Q, Chen J, Tian L. MicroRNA-7 inhibits tumor growth and metastasis by targeting the phosphoinositide 3-kinase/Akt pathway in hepatocellular carcinoma. *Hepatology*. 2012;55(6):1852–1862. doi:10.1002/hep.25576
33. Zhang X, Hu S, Zhang X, et al. MicroRNA-7 arrests cell cycle in G1 phase by directly targeting CCNE1 in human hepatocellular carcinoma cells. *Biochem Biophys Res Commun*. 2014;443(3):1078–1084. doi:10.1016/j.bbrc.2013.12.095